Effect of Iron Impurity in Zinc Sulfide Concentrates on the Rate of Dissolution

The rate of dissolution of sphalerite is shown to be directly proportional to the concentration of substitutional iron impurity in the solid. This is attributed to the formation of a narrow impurity band within the forbidden band gap of the sphalerite. The impurity band is of iron *d*-orbital origin. The transfer of electrons between this *d*-orbital band and the oxidant is energetically more favorable than the transfer of electrons between the valence band and the oxidant. A fundamental model combining the electronic structure of sphalerite and semiconductor electrochemistry is presented. An equation is derived that describes the rate of dissolution as being first order for the concentration of iron in the solid and half-order for the concentration of the oxidant. This is in agreement with the experimental evidence.

Frank K. Crundwell
Council for Mineral Technology (MINTEK)
Randburg, 2125, South Africa

Introduction

The stringent environmental restrictions imposed on sulfide smelters have led to the development of hydrometallurgical routes for the extraction of metal sulfides that avoid the production of sulfur dioxide. These processes involve the aqueous oxidation of sulfide to elemental sulfur or to sulfate by an oxidant such as ferric ion or dissolved oxygen. In particular, considerable attention has been focused on the development of processes for the leaching of zinc sulfide concentrates in chloride and sulfate solutions using dissolved iron (III) as the oxidant (Jin and Warren, 1985; Verbaan and Crundwell, 1986; and references therein).

The rate of dissolution of a solid, such as sphalerite, in aqueous solutions depends on the processes occurring at the solid-solution phase boundary. These processes include, among others, the formation of complexes, the transfer of charge, and the adsorption of ions at the surface. The dissolution process can be classified on the basis of the rate-determining step, for example, mass transfer, chemical reaction, or charge transfer.

The rate-determining step in many dissolution reactions is a *charge-transfer* step, and the oxidative dissolution of sulfide minerals includes such an electrochemical reaction in which the sulfide mineral is oxidized and the oxidant reduced at the mineral surface. The mixed-potential model, developed to describe metallic corrosion processes, has gained acceptance in research on leaching and flotation, and was recently used to describe the kinetics of the oxidative dissolution of sphalerite. This model successfully describes the half-order dependence of the rate of dissolution on the concentration of oxidant in solution (Jin and Warren, 1985; Verbaan and Crundwell, 1986; Crundwell, 1987). This application of this model assumes that electron transfer is the rate-controlling step, that the mechanism of dissolution is analogous to the metallic corrosion process, and that the sphalerite behaves like a corroding metal. However, many sulfide minerals are semiconductors, and it is well known that the electronic properties of semiconductors, such as the band structure and the impurities, influence the rate of dissolution (Simkovich and Wagner, 1960; Eadington and Prosser, 1969).

The rate at which iron-containing sphalerites, (Zn, Fe)S, are oxidatively dissolved is known to be higher than that of pure ZnS (Exner et al., 1969), and Piao and Tozawa (1985) reported that the rate of reaction is linearly proportional to the concentration of substitutional iron in the zinc sulfide lattice. Pawlek (1969) proposed that the cathodic reduction of oxygen would vary with the number of charged carriers, in support of which he found that the irradiation of sphalerite with UV energy caused an appreciable increase in the rate of dissolution. The results of Exner et al. (1969), Pawlek (1969), and Piao and Tozawa (1985) indicate the electronic structure is important in the dissolution of sphalerite, because of the influence of the iron content of the (Zn, Fe)S solid solution, and the influence of UV irradiation. (In the dissolution of any concentrated mineral there is also the possibility that galvanic interactions might increase or decrease the rate of reaction because concentrate is not well liberated.)

This paper explores the influence of the electronic structure of (Zn, Fe)S on the rate of dissolution. The solid-state properties of

sphalerite are reviewed, and the principles of semiconductor electrochemistry are summarized. These two considerations are combined in a derivation that describes the dissolution of (Zn, Fe)S. This equation correctly describes the effect of the iron impurity in the sphalerite and the effect of the concentration of the oxidant in the solution. This model justifies the previous use of the mixed-potential model, and describes the dependence of the rate of reaction on the oxidant concentration and on the concentration of iron impurity in the sphalerite.

Experimental results are presented that confirm the results of Piao and Tozawa (1985), even though ferric chloride was used as the oxidant instead of oxygen. An electrochemical model would usually be verified by fundamental electrochemical techniques using an electrode. Since sphalerite is unsuitable for use as an electrode in conventional electrochemical experiments because of its high resistivity, mixtures of sphalerite and graphite have been used as electrodes (Scott and Nicol, 1978; Gerlach and Kuzeci, 1984; Guerrette and Ghali, 1985). The graphite serves to lower the resistivity of the electrode, so that the applied potential appears across the Helmholtz layer. However, Scott and Nicol reported that the presence of graphite in contact with sphalerite altered the mechanism of reaction, a fourfold to fivefold increase in the rate of reaction being obtained for a sphalerite-graphite electrode over that of a sphalerite-PTFE electrode. Guerette and Ghali (1985) reported similar results: the anodic behavior of compacted sphalerite-graphite mixtures is different from that of uncompacted samples. For these reasons, batch leaching tests were used to provide confirmation of the proposed electrochemical model.

Solid-State Properties of (Zn, Fe)S

Zinc sulfide exists as two polytypes: the hexagonal type (wurtzite) and the cubic type (sphalerite), which is more abundant. Both polytypes are semiconductors of intermediate ionicity, with a band gap—determined by optical measurement and quantum calculation—in the range 3.6 to 3.9 eV (Vaughan and Craig, 1978). Chemical bonding indicates that the bottom of the conduction band is derived from the zinc 4*s*-orbital, while the top of the valence band is derived primarily from the sulfur 3*p*-orbital (Shuey, 1975). This is in qualitative agreement with the ionic model, which associates the valence band with the anion, sulfur, and the conduction band with the cation, zinc (Mott and Gurney, 1948).

Zinc sulfide is such a poor electrical conductor that it is often classified as an insulator and resistivities in the range 10^7–10^9 $\Omega \cdot$ cm have been reported. The mechanism of intrinsic conduction in zinc sulfide may be p- or n-type, depending on the stoichiometry. Telkes (1950) obtained high positive thermopowers, indicating p-type conduction for four samples of sphalerite. This, however, may have been due to the presence of iron impurity, giving rise to conduction in a *d*-orbital band (Keys et al., 1968).

The substitution of transition metal impurities for zinc in zinc sulfide has a pronounced effect on the electrical properties. Measurements of the electrical conductivity of a natural sphalerite with an iron content of 12.4 atom % showed that sphalerite exhibited typical semiconductor behavior, with an activation energy for conduction of 0.49 eV, although its electrical resistivity was high at $8 \times 10^7\ \Omega \cdot$ cm (Keys et al., 1968). The absence of a measurable Hall effect and a positive thermoelectric power (Telkes, 1950) suggest the hopping of holes in a localized *d*-orbital band as the conduction mechanism (Vaughan and Craig, 1978; Keys et al., 1968). This model requires the holes to be generated as Fe^{3+} ions, i.e., the absence of one *d*-orbital electron is necessary, although only one in 800 iron atoms need be Fe^{3+} in order to account for the conductivity (Keys et al., 1968).

Quantum calculations indicate that the $2e$ and $4t_2$ orbital levels are about 0.56 and 1.44 eV above the valence band, respectively (Majewski, 1981). These calculations give evidence of bond formation involving the iron impurity and the host ligands. The $2e$ and $4t_2$ orbitals can be represented as a localized band within the zinc sulfide band gap, and the removal of electrons from either of these orbitals will create the holes required for the *d*-orbital conduction mechanism. The two other elements that substitute for zinc are cadmium and manganese, both of which have no effect on the electrical conductivity (Shuey, 1975).

Energy Level Model of Semiconductor Electrochemistry

The immersion of a solid in an electrolyte redistributes the charge at the interface, so that an excess of charge density in the electrolyte is balanced by an equal density of charge in the solid (the space-charge layer) at equilibrium (Mehl and Hale, 1966; Gerischer, 1970; Morrison, 1980). The band model of a semiconductor, which is characterized by the band gap between the valence and conduction bands, differs from that of a metal primarily because of this space-charge layer. The excess charge density in the space-charge region results in a "band bending" at the solid-liquid interface. A downward band bending occurs if the surface is negatively charged; upward band bending occurs if it is positively charged.

Energy levels at the interface have a substantial influence on the interactions at the solid-liquid interface, and the capture of electronic carriers at the solid surface is a dominating influence in electrochemical corrosion (Morrison, 1980). Electron transfer can occur only between states of the same energy level (Gurney, 1931), i.e., when there is no transfer of energy with the surroundings, or radiation.

Figure 1 compares the energy levels of the bands of (Zn, Fe)S with those of the ions in solution. The energy levels of the valence and conduction bands at the point of zero charge, E_{vs} and E_{cs} respectively, were calculated by the method of Butler and Ginley (1978). The band edges for a number of other sulfides and the energy levels of a number of redox couples are also shown.

The energy levels of an ion in solution are distributed as a result of the thermal fluctuation of the dipoles in the solvation sheath surrounding the ion. Theories of electrostatic polarization (Marcus, 1964; Levich, 1970) indicate that the distribution of energy levels is Gaussian. Figure 1 illustrates this model for the ferricyanide and ferrocyanide ions. The probability of electron transfer between an electrode and an ion in solution will depend on the energy level of the ion at the instant of transfer, so these fluctuations are important (Marcus, 1964). The energy needed for an ion to reach the activated state is the difference between the energy of the oxidizing agent, E_{ox}, and the activation-state energy, E^*. The probability, W_{ox}, that the energy level of a species will be at E^* is given by

$$W_{ox} = (4\pi\lambda kT)^{-1/2} \exp\left[-(E_{ox} - E^*)^2/4\pi kT\right] \qquad (1)$$

where k is the Boltzmann constant, T is temperature, and λ is

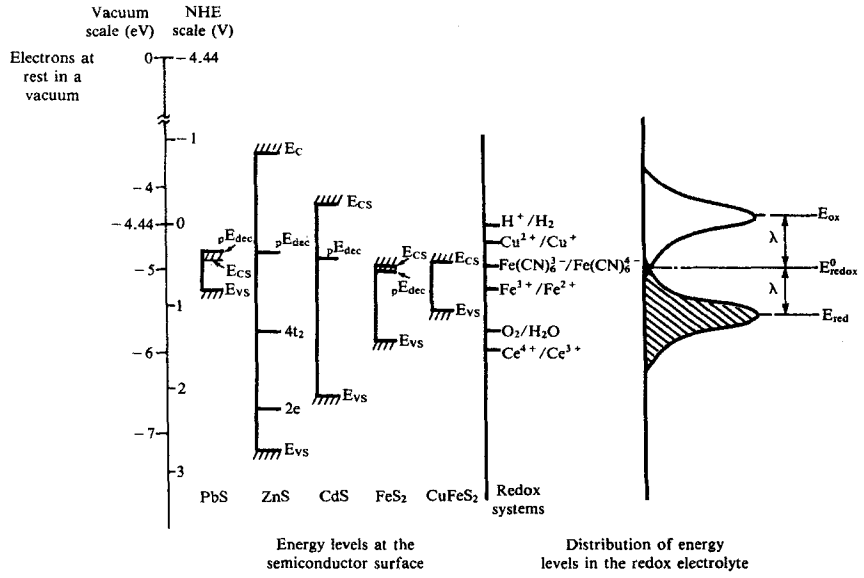

Figure 1. Energy levels at semiconductor surface for various mineral sulfides, and energy levels of oxidants in aqueous solutions.

Scale at left shows both vacuum and hydrogen energy scales
E_{cs}, E_{vs}: conduction and valence-band edges, respectively
$4t_2$, $2e$: iron d-orbital levels in ZnS
p^E_{dec}: thermodynamic decomposition potential

the reorganization energy, which includes the energy contributions from the stretching of bonds in the inner coordination sphere, and the rotation of solvent molecules in the outer sphere (Marcus, 1964; Bockris and Khan, 1985).

These fluctuations in energy are not small, and the standard deviation $(\lambda kT)^{1/2}$ can be several tenths of an electron volt (Morrison, 1978).

The location of the energy levels of ions in solution can be obtained from the standard potential of the redox couple. E°_{redox}, equal to $\frac{1}{2}(E_{red} + E_{ox})$, is related directly to the potential tabulated in handbooks (Morrison, 1978). The levels of the ions on the vacuum energy scale are shown in Figure 1.

Experimental Method

Samples of five sphalerites were used in the present study. All samples were wet-screened, and a sample in a narrow size range was selected. This fraction was first washed with Na_2S to remove flotation reagents, and with dilute sulfuric acid. The origin, chemical composition, and mean particle size of each sample are given in Table 1. The Ward's sample is a natural pure sphalerite (museum grade), which is honey-colored. Mineralogical analyses were carried out on the samples as received, and are shown in Table 2. The iron content of each sphalerite was determined by electron-microprobe analysis of about 100 particles. The results of this examination are given in Table 3.

The reactor consisted of a 1 L cylindrical glass vessel with a flat Perspex impeller driven by a variable speed motor. A single Perspex baffle was installed. The temperature was maintained to within 0.5°C by a contact thermometer connected to one of the ports in the lid. A solution bridge connected a calomel reference electrode to the solution, and the redox potential was measured by use of a platinum electrode. All potentials reported here refer to the saturated calomel electrode (SCE) unless otherwise stated. The redox potential was maintained to within 2 mV by the addition of 3% hydrogen peroxide, the amount of the addition being controlled by a Radiometer PHM84/TTT80 titrator system. The pH of the solution, which was measured with a combined glass and Ag/AgCl reference electrode, was maintained to within 0.1 units in the pH range 1 to 1.5 by the addition of hydrochloric acid (500 g · L^{-1}). The pH was controlled by a system similar to that used for control of the redox potential. A Phillips 125 W UV lamp was used to irradiate the leaching vessel.

The standard conditions used in this study were as follows. The leaching solution consisted of an aqueous solution of 0.2 M $FeCl_3$, 0.3 M HCl, 0.005 M $FeCl_2$, 2 M NaCl. The standard temperature was 65°C. Distilled water and analytical reagent grade chemicals were used. A high concentration of chloride was chosen to prevent the formation of a film of insoluble lead

Table 1. Chemical % Compositions of Sphalerite Concentrates

	Origin of Sphalerite				
	Ward's	Zincor	Black Mountain	Rosh Pinah	Gamsberg
Zn	66.5	56.7	49.8	56.7	51
S	32.2	32.6	28.6	30.1	28.8
Fe	0.5	7.25	9.72	4.35	9.08
Cu	0.038	0.018	0.37	0.25	0.14
Pb	0.090	1.51	3.46	1.46	0.74
Cd	0.48	0.12	0.138	0.12	0.087
Mn	0.005	0.01	1.26	0.29	2.34
Geomet. mean particle size, μm	48.8	68.7	44.8	44.8	44.8

Table 2. Mineralogical % Compositions of Sphalerite Concentrates

	Origin of sphalerite				
	Ward's	Zincor	Black Mountain	Rosh Pinah	Gamsberg
Sphalerite	100	88.9	97.4	92.2	98.8
Chalcopyrite + covellite	trace	trace	trace	0.2	nd
Galena	trace	0.5	0.4	trace	nd
Pyrite + pyrrhotite	trace	7.5	1.4	7.4	1.2
Silicate gangue minerals	nd	3.1	0.8	0.2	nd

nd: Not Detected

sulfate on the surface of the concentrates with a high galena content (Crundwell, 1987). Once the initial conditions had stabilized, 1.5 g of concentrate was rapidly added to 0.75 L of solution. A low solid-to-liquid ratio was chosen so that the addition of hydrogen peroxide and hydrochloric acid during the reaction would not change the total volume of the solution to a significant extent.

Samples of solution were taken during the reaction with a 15 mL syringe, and filtered immediately under vacuum. The concentration of zinc in solution was determined by atomic absorption spectrophotometry, and the addition of hydrogen peroxide during the reaction was monitored as a check on the zinc concentration in solution, and was always found to be stochiometrically proportional to the zinc concentration. Direct oxidation of the sphalerite by hydrogen peroxide was assumed to be minomal due to the low solid-liquid ratio, and the fast oxidation reaction with Fe(II).

Results

If it is assumed that a surface reaction controls the rate of dissolution, then the shrinking particle model is applicable. This has the following form for spherical particle geometry:

$$k_r t = 1 - (1 - X)^{1/3} \tag{2a}$$

$$k_r = k_s f(C_{ox})/\rho_b r_o \tag{2b}$$

where X is the conversion of zinc in the solid to zinc in solution, k_s is a rate constant, $f(C_{ox})$ is a function of the concentration of oxidant C_{ox}, ρ_b is the molar density, r_o is the initial particle radius, k_r is a constant, and t is the time elapsed.

Typical results collected in the study and presented in Figure 2 as a plot of $1-(1-X)^{1/3}$ against t, illustrate the effect of the iron

Table 3. Iron Content in (Zn, Fe)S Mineral Phase

Sphalerite	Fe in (Zn, FE)S %
Ward's	0.55
Zincor	2.56
Black Mountain	8.02
Rosh Pinah	1.79
Gamsberg	8.62

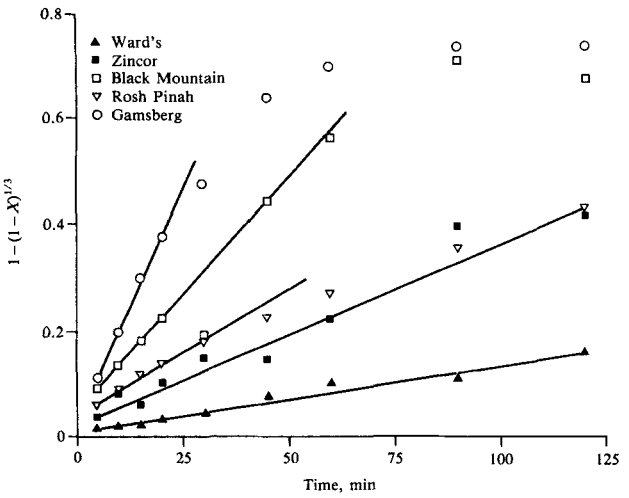

Figure 2. Plot confirming shrinking particle model for dissolution of sphalerite concentrates.
Dissolution at 65°C in ferric chloride solutions: 0.2 M $FeCl_3$, 0.3 M HCl, 0.005M $FeCl_2$, 2 M NaCl

content of the different sphalerite concentrates on the rate of dissolution. The diagram shows that the reaction follows linear kinetics in the initial stage of the reaction, while diffusion through the product layer is important in the latter stage. The value of k_r is obtained from the slope of the linear section of these diagrams. In order to eliminate the effect of the difference in the size of the particles, values of $k_r r_o$ are compared.

The effect of temperature on the rate of dissolution of the five sphalerite concentrates is shown in Figure 3 as an Arrhenius plot. The activation energies evaluated from this diagram are given in Table 4. No dependence of the activation energy on the iron content is apparent.

Figure 4 illustrates the effect of the iron content of the sphalerite concentrates on the rate of dissolution at three different temperatures. These results confirm the linear variation reported by Piao and Tozawa (1985), who used oxygen as an oxidant. The use of a different oxidant does not affect the dependence of the rate on the iron content of the sphalerite.

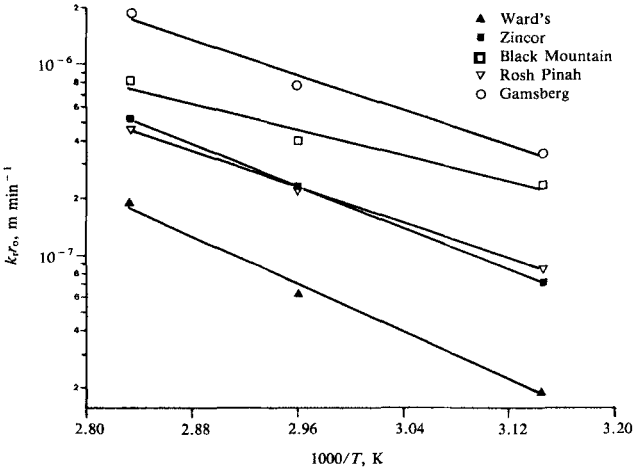

Figure 3. Arrhenius plot for dissolution of sphalerite concentrates.
FeCl solutions as in Figure 2

Table 4. Activation Energies for Leaching of Sphalerites

Sphalerite	E_a kJ · mol^{-1}
Ward's	59.5
Zincor	51.6
Black Mountain	31.7
Rosh Pinah	44.1
Gamsberg	43.3

The dissolution of the sphalerite from Black Mountain is consistently lower than that expected from the straight-line variation in iron content, and this, together with its significantly lower activation energy, suggests that other sulfides present as inclusions in the sphalerite galvanically protect the sphalerite, or that a protective coating develops on the particle surface. This is most noticeable at higher temperatures.

The introduction of different oxidizing agents is illustrated in Figure 5, and the effect of UV radiation is shown in Figures 6 and 7. The energy barrier between the *d*-band and the oxidizing agent is smaller for ceric ion than for ferric ion (see Figure 1), and the rate of reaction is dramatically increased by the use of ceric ion as the oxidant. An oxidant with an E^o_{redox} lower than the iron couple may not be able to produce fluctuations in energy that have a significant overlap with the *d*-band, and electron transfer will be slow or will not take place at all. This is the case when stannic chloride is used as an oxidant and virtually no dissolution occurs. (The stannous/stannic and the cuprous/cupric couples have E^o_{redox} of 0.15 and 0.19 V, respectively, and the energy level of the stannous/stannic couple is close to that of the cupric/cuprous couple shown in Figure 1.)

The radiation of a sample undergoing anodic dissolution results in enhanced rates of leaching, although this is not as pronounced as was reported by Exner et al. (1969). These results confirm the importance of semiconductor and other solid-state considerations in the dissolution of iron-containing sphalerites.

Discussion

In semiconductors with wide band gaps ($E_{gap} > 1$ eV), oxidation occurs as a result of the injection of holes into the valence band (Morrison, 1978); oxidation by surface holes will occur with 100% corrosion efficiency. However, Figure 1 shows that the injection of holes into the narrow *d*-orbital band is energetically more favorable than injection into the valence band. Large numbers of these holes can exist at the surface, resulting in a narrow space-charge region. If the space-charge region is sufficiently narrow (≈2 nm), quantum tunneling can occur between the surface *d*-orbital band and the valence band. The capture of two holes by the valence band at the surface will result in the oxidation of S^{2-} associated with the valence band to S^0 and the concomitant release of zinc associated with the conduction band into solution as Zn^{2+}(aq) (Williams, 1960; Koch, 1975). The electronic processes occurring during the dissolution of sphalerite are

$$ZnS + 2h^+ \rightarrow Zn^{2+} + S^0 \quad (3)$$

$$ox \rightarrow red + h^+ \quad (4)$$

where h^+ represents a hole in the valence band, *ox* an oxidant in solution, and *red* a reductant in solution.

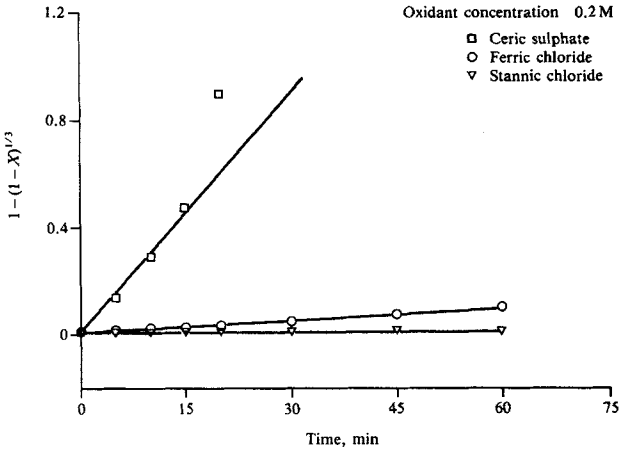

Figure 5. Effect of different oxidants on rate of dissolution of Ward's sphalerite.

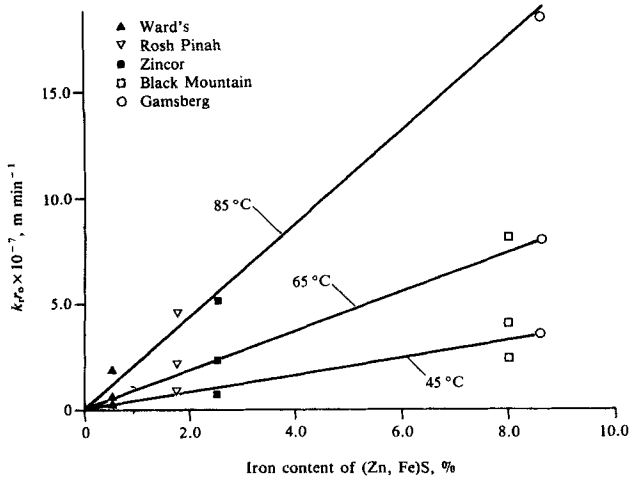

Figure 4. Effect of iron content of (Zn, Fe)S on rate of dissolution.
FeCl solutions as in Figure 2

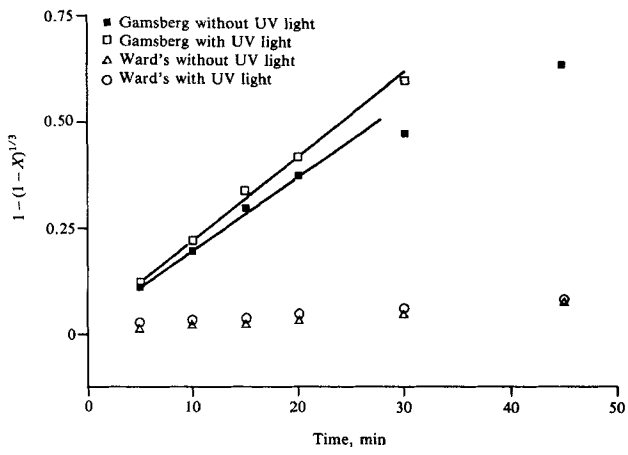

Figure 6. Effect of UV radiation on rate of anodic dissolution for Ward's and Gamsberg sphalerites.
Solutions as in Figure 2, 65°C

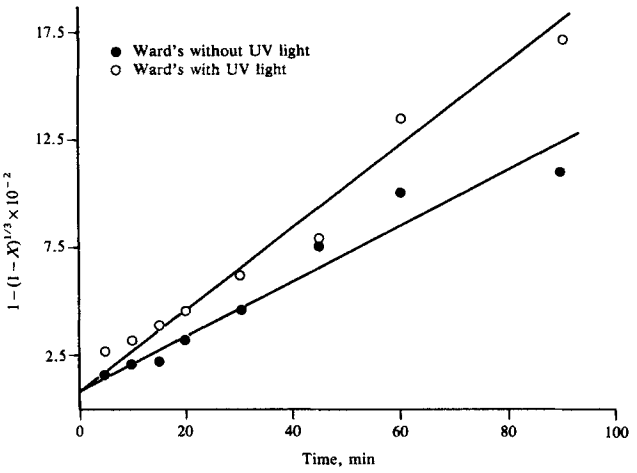

Figure 7. Effect of UV radiation on rate of anodic dissolution for Ward's sphalerite.
Solutions as in Figure 2, 65°C

The rate of electron transfer from the semiconductor to the solution is proportional to the number of occupied states in the semiconductor, $D_{sc}(E)f(E - E_{sc})$ and the number of unoccupied states in the redox electrolyte, $D_{ox}(E)$, at the same energy, E. $D_{sc}(E)$ is the density of states in the semiconductor, $f(E - E_{sc})$ is the Fermi function describing how many of these states are occupied, and $D_{ox}(E)$ is the density of states in the oxidizing agent in solution. The total current from the semiconductor to the electrolyte is the integral of this probability over all possible energy levels (Gerischer, 1970)

$$j^- = q\int_{-\infty}^{\infty} \nu^-(E)D_{sc}(E)f(E - E_{sc})D_{ox}(E)\,dE \qquad (5)$$

where $\nu^-(E)$ is the transmission coefficient, and q is the electronic charge. The presence of an iron d-orbital within the band gap has two consequences for electron transfer between the solid and the electrolyte: it presents a narrow localized band with which the transfer of electrons is energetically more favorable than it is with the valence band, and it "pins" the Fermi level at a level within the d-orbital band (Jellinek, 1972; Bard et al., 1980).

The first consequence of the iron impurity is that electron transfer occurs between the narrow d-orbital band within the semiconductor and the electrolyte. This means that the density of states for the carriers in the solid resembles a Dirac-delta function of density centered on the energy of the band with a magnitude of N_d (Mehl and Hale, 1966). The transmission coefficient $\nu^-(E)$ also has the form of a Dirac delta function, and since $D_{ox}(E) = C_{ox}W_{ox}(E)$, Eq. 5 can be evaluated if it is assumed that the overlapping of states is limited to a rather small range, i.e., charge transfer will occur within 1 kT of the edge of the impurity band (Gerischer, 1970). If this is the case, it is reasonable to replace the integral by substituting $\Delta E = 1\ kT$ and $W(E) = W(E^*)$ where E^* denotes the energy at which charge transfer occurs at the surface, i.e., the energy of the d-orbital band. Therefore,

$$j^- \approx qzN_dC_{ox}W_{ox}(E^*)kT$$
$$= qz(kT/4\pi\lambda)^{1/2}\exp\left[-(E_{ox} - E^*)^2/4\lambda kT\right] \qquad (6)$$

where N_d is the concentration of occupied states in the d-band and C_{ox} is the concentration of oxidant in solution.

The second consequence of the iron impurity is that the Fermi level, E_F, is pinned at the level of the d-orbital band. Hence, the change in potential appears across the Helmholtz layer, i.e., $E^* = E_F$, and $E_{ox} - E_F$ varies directly with applied voltage given by the overpotential, η. This means that

$$E_{ox} - E^* = E_{ox} - E_F = E_{ox} - E_{F,o} + \eta q \qquad (7)$$

where η is the overpotential. Substituting Eq. 7 into Eq. 6 gives the cathodic reduction of Fe^{3+} as

$$j^- = q(kT/4\pi\lambda)^{1/2}C_{ox}N_d$$
$$\cdot \exp\left[-(E_{ox} - E_{F,o} + \eta q)^2/4\lambda kT\right] \qquad (8)$$

Since $E_{ox} - E_{red} = 2\lambda$ and $E_{F,o} = \frac{1}{2}(E_{ox} + E_{red}) + kT\ln(C_{red}/C_{ox})$ (Gerischer, 1970),

$$E_{F,o} - E_{red} = \lambda + kT\ln(C_{red}/C_{ox}) \qquad (9)$$

and

$$j^- = qzN_dC_{ox}$$
$$\cdot \exp\left[-(\lambda - kT\ln(C_{red}/C_{ox}) + \eta q)^2/4\lambda kT\right] \qquad (10)$$

If the assumptions of Marcus (1964) and Levich (1970), i.e., $\lambda \gg q\eta$ and $\lambda \gg kT\ln(C_{red}/C_{ox})$, are applied the cross terms in $q\eta$ and $kT\ln(C_{red}/C_{ox})$ can be neglected. The resulting equation describes the reduction of Fe^{3+} at the sphalerite surface, i.e.,

$$j^- = k_{-1}C_{ox}N_d\exp(-\eta q/2kT) \qquad (11)$$

where k_{-1} is a rate constant. The anodic dissolution current is also dependent on the number of point defects (Simkovich and Wagner, 1960):

$$j^+ = k_1N_d\exp(\eta q/2kT) \qquad (12)$$

The overpotential, η, in Eqs. 11 and 12 appears across the Helmholtz layer because the Fermi level is pinned. Since $j^- = j^+$ Eqs. 11 and 12 can be equated, and an expression for η can be obtained in a way that is analogous to the mixed-potential model. Then solving for j^+ gives

$$j^+ = k_1N_d(C_{ox}k_{-1}/k_1)^{1/2} \qquad (13)$$

This is first order in N_d, the number of occupied states in the d-band, i.e., the concentration of iron in substitutional lattice sites, and half-order in the concentration of oxidant. This equation is capable of describing all the experimental results reported in the literature (Piao and Tozawa, 1985; Jin and Warren, 1985) and is confirmed by the results presented in Figure 4. For a particular sphalerite, the dependence of the rate on the oxidant concentration from Eq. 13 is the same as that described by the mixed-potential model. Indeed, the fact that the Fermi level is pinned justifies the use of the mixed-potential model for a semiconductor such as sphalerite.

From the energy level model of semiconductor electrode processes (Morrison, 1978), it is expected that the dissolution rate would be enhanced by the introduction of a stronger oxidizing

agent, i.e., a higher E_{ox}, or by ultraviolet radiation (band gap energy), which would create free electrons in the conduction band and holes in the valence band. Such photoeffects are expected even if the Fermi level is pinned.

Exner et al. (1969) investigated the effect of UV radiation on the dissolution rate of both natural and synthetic zinc sulfide crystals and found that UV radiation dramatically increased the rate of dissolution for synthetic doped crystals, suggesting that n-type doping predominated. A smaller effect was reported for pure natural crystals. These results confirm the importance of the electronic structure of the solid.

The results of Jin and Warren (1985) show that there is a change in the reaction order, from half-order to zero order at high oxidant concentration. Jin and Warren, and Van Sandvijk and Koopmans (1986), proposed models for which they assumed that the oxidant is adsorbed onto the surface, and described this adsorption using the Langmuir isotherm. Therefore, those authors attributed the change in reaction order to the onset of complete coverage of the surface by the adsorbed oxidant.

The model presented in this paper is in contrast to the adsorption models previously proposed. Metal ions in aqueous solution are solvated, the significance of which is that such ions are seldom adsorbed at the inner Helmholtz plane (IHP). Solvated ions, such as $Fe^{3+}(aq)$, are electrostatically adsorbed at the outer Helmholtz plane (and an outer sphere electron-transfer reaction occurs). This is not identical to adsorption at a specific site, which is a requirement for the application of the Langmuir isotherm. The change in reaction order that those authors are attempting to describe suggests that the anodic dissolution current, Eq. 12, reaches a limiting value because of a migration-limited supply of solid-phase charge carriers (electrons or holes) to the surface. The limiting current is constant for any change in the applied potential or in the oxidant concentration. Such limiting currents are a fundamental aspect of the anodic behavior of n-type semiconductors, and this proposal is consistent with the characteristics of semiconductor electrochemistry and the model represented by Eqs. 11, 12, and 13.

Conclusions

The dissolution of sphalerite has been described by a fundamental model that combines the considerations of the structure of (Zn, Fe)S and of semiconductor electrochemistry. An equation has been derived that describes the known features of the dissolution of sphalerite. This equation assumes that transfer of electrons takes place between the iron-impurity *d*-orbital band in the band gap of the sphalerite and the oxidant in solution. This model predicts the observed first-order dependence of the dissolution rate on the concentration of iron in the sphalerite and its half-order dependence on the concentration of oxidant in solution. Experimental results are presented that confirm previous experimental investigations and the form of the equation derived for the anodic dissolution of sphalerite.

Literature Cited

Bard, A. J., A. B. Bocarsly, F-R. Fan, E. G. Walton, and M. S. Wrighton, "The Concept of Fermi Level Pinning at Semiconductor/Liquid Junctions," *J. Am. Chem. Soc.*, **102,** 3671 (1980).

Bockris, J.O'M., and S. U. Khan, "On the Evolution of Concepts Concerning Events at the Semiconductor/Solution Interface," *J. Electrochem. Soc.*, **132,** 2648 (1985).

Butler, M. A., and D. S. Ginley, "Prediction of the Flat Band Potentials at Semiconductor Interfaces from Atomic Electronegativities," *J. Electrochem. Soc.*, **125,** 228 (1978).

Crundwell, F. K., "Kinetics and Mechanism of the Oxidative Dissolution of a Zinc Sulfide Concentrate in Ferric Sulfate Solutions," *Hydromet.*, **19,** 227 (1987).

Eadington, P., and A. P. Prosser, "Oxidation of Lead Sulfide in Aqueous Suspensions," *Trans. Inst. Min. Metall.*, **78,** c74 (1969).

Exner, F., J. Gerlach, and F. Pawlek, "Pressure Leaching of Zinc Sulfide," *Erzmetall,* **22,** 219 (1969).

Gerischer, H., "Semiconductor Electrochemistry," *Physical Chemistry: An Advanced Treatise,* H. Eyring et al., eds., Academic Press, New York, vol. 9A (1970).

Gerlach, J., and E. Kuzeci, "Electrochemical Behavior of Zinc Sulfide in Graphite Paste," *Erzmetall,* **37,** 261 (1984).

Guerrette, C., and E. Ghali, "The Anodic Dissolution of ZnS-Graphite Mixture in a Dilute Hydrochloric Acid Solution," *Proc. Int. Symp. Extractive Metall. of Zinc,* K. Tozawa, ed., Min. Metall. Inst. Japan, Tokyo (1985).

Gurney, R. W., "Quantum Mechanics of Electrolysis," *Proc. Roy. Soc. Lond.,* **A134,** 137; **A136,** 378 (1931).

Jellinek, F., in *International Review of Science, Transition Metals,* Pt. 1, D. W. A. Sharpe, ed., Inorganic Chem. Ser. 1, vol. 5, Butterworths, London (1972).

Jin, Z-M., and G. W. Warren, "Reaction Kinetics and Electrochemical Model for the Ferric Chloride Leaching of Sphalerite," *Proc. Int. Symp. Extractive Metall. Zinc,* K. Tozawa, ed., Min. Metall. Inst. Japan, Tokyo (1985).

Keys, J. D., J. L. Horwood, T. M. Baleshta, L. J. Cabri, and D. C. Harris, "Iron-Iron Interaction in Iron-Containing Zinc Sulfide," *Can. Mineral.,* **9,** 453 (1968).

Koch, D. F. A., "Electrochemistry of Sulfide Minerals," *Modern Aspects of Electrochemistry,* **10,** J. O'M. Bockris, B. E. Conway, eds., Plenum, New York (1975).

Levich, V. G., in *Physical Chemistry: An Advanced Treatise,* **9A** H. Eyring et al., eds., Academic Press, New York, (1970).

Majewski, J. A., "Electronic Structure of Transition Metal Impurities in Zinc Sulfide," *Phys. Stat. Sol. B,* **102,** 663 (1981).

Marcus, R. A., "On the Theory of Electron-Transfer Reactions," *Ann Rev. Phys. Chem.,* **15,** 155 (1964).

Mehl, W., and J. M. Hale, "Insulator Electrode Reactions," In *Adv. in Electrochem. and Electrochem. Engg.,* **6,** C. W. Tobias, P. Delahay, eds., Interscience, New York (1966).

Morrison, S. R., *Electrochemistry at Semiconductor and Oxidized Metal Electrodes,* Plenum, New York (1980).

———, "Study of Semiconductors Using Electrochemical Techniques," *J Vac. Sci. Technol.,* **15,** 1417 (1978).

Mott, N. F., and R. W. Gurney, *Electronic Processes in Ionic Crystals,* 2nd ed., Oxford, New York (1948).

Pawlek, F., "Research in Pressure Leaching," *J. S. Afr. Inst. Min. Metall.,* **69,** 632 (1969).

Piao, S. Y., and K. Tozawa, "Effect of Iron Content in Zinc Sulfide Concentrates on Zinc Extraction," *J. Min. Metall. Inst. Japan,* **101,** 795 (1985).

Scott, P. D., and M. J. Nicol, "The Kinetics of the Leaching of Zinc Sulfide Concentrates in Acidic Sulfate Solutions," Rept. 1949, Council for Mineral Technology, Randburg (1978).

Simkovich, G., and J. B. Wagner, "The Influence of Point Defects on the Kinetics of Dissolution of Semiconductors," *J. Electrochem. Soc.,* **110,** 513 (1960).

Shuey, R. T., *Semiconducting Ore Minerals,* Elsevier, Amsterdam (1975).

Telkes, M., "Thermoelectric Power and Electrical Resistivity of Minerals," *Am. Mineral.,* **35,** 536 (1950).

Van Sandwijk, A., and K. Koopmans, "An Adsorption Model for the Leaching of Sphalerite by Iron (III) Chloride in Hydrochloric Acid Solutions," *Delft Prog. Rept.,* **11,** 33 (1986).

Vaughan, D. J., and J. R. Craig, *Mineral Chemistry of Metal Sulfides,* Cambridge, London (1978).

Verbaan, B., and F. K. Crundwell, "An Electrochemical Model for the Leaching of a Sphalerite Concentrate," *Hydrometall.,* **16,** 345 (1986).

Williams, R., "Becquerel Photovoltaic Effect in Binary Compounds," *J. Chem. Phys.,* **32,** 1505 (1960).

Manuscript received Oct. 19, 1987, and revision received Feb. 3, 1988.